

Wake field in dielectric acceleration structuresL. Schächter,¹ R. L. Byer,² and R. H. Siemann³¹*Department of Electrical Engineering, Technion-IIT, Haifa 32000, Israel*²*Department of Applied Physics, Stanford University, Stanford, California 94305-4085, USA*³*SLAC, Stanford University, Stanford, California 94305-4085, USA*

(Received 20 November 2002; revised manuscript received 5 March 2003; published 5 September 2003)

In this study we present a general approach for the analysis of the wake field of a point charge moving in a vacuum tunnel bored in dielectric material that is uniform in the direction parallel to the motion of the bunch. In the transverse direction the structure surrounding the dielectric may have arbitrary geometry. A quasianalytic expression that relates the decelerating force with the first dielectric layer, the radius of the vacuum tunnel where the charge moves, and the reflection characteristics of the structure has been developed. Simulation results for a simple structure indicate that, if the effective location where the reflection occurs in the dielectric is sufficiently apart from the edge of the vacuum tunnel, it has no effect on the point charge. In fact, the decelerating field converges exponentially as this distance increases, to the asymptotic value determined by the first dielectric layer. An estimate of the trailing wake when the structure supports a specific mode is also provided.

DOI: 10.1103/PhysRevE.68.036502

PACS number(s): 41.75.Lx, 41.20.Jb, 41.60.Bq

I. INTRODUCTION

One of the appealing paradigms for future particle accelerators relies on dielectric slow-wave structures confining a laser field. Conceptually, this is quite similar to today's linear accelerators driven by microwave sources. Efforts are under way [1] for a proof of principle at the level of the interaction of electrons with a laser field in a single cell, but eventually any practical accelerator will consist of a series of extended slow-wave structures that need to satisfy several conditions. Beyond slowing down the phase velocity to the speed of light, it needs to ensure a maximum longitudinal electric field at the location of the electrons for a given laser power, minimize dissipation loss, and provide good heat transfer characteristics. Moreover, in order to avoid breakdown it is important to ensure minimum electric field at the vacuum interface as well as in the dielectric, entailing a need for some trade-off between the latter and the need for maximum power imposed by the maximum gradient condition. At the high intensities involved, the laser field may affect the dielectric coefficient of the structure (optical Kerr effect) thus altering the wave's phase relative to the accelerated bunch. Finally, when a bunch is injected into a dielectric acceleration structure, its deceleration ought to be as small as possible. It is the wake field that is responsible for this decelerating field, and it is its analysis that is the focus of the current study.

Throughout the years extended studies of wake fields have been conducted, many of which have been summarized in reviews by Heifets and Kheifets [2] and Chao [3]. However, the large majority of these studies address wakes in azimuthally symmetric metallic disk-loaded structures or metallic cavities used in microwave accelerators which have only limited relevance to optical dielectric structures. In the study that follows, a general approach is being developed for estimation of the impact of a dielectric structure that is uniform in the direction parallel to the moving charge and has virtually arbitrary characteristics in the transverse directions.

We present a quasianalytic expression that relates the decelerating force to the first dielectric layer of the structure, the radius of the vacuum tunnel where the charge moves, and the reflection characteristics of the structure.

II. PRIMARY FIELD

Whatever structure surrounds the vacuum tunnel where the electron bunch propagates, it can be represented mathematically by a matrix that relates the outgoing waves with the incoming ones. The top frame of Fig. 1 illustrates the conceptual configuration of a vacuum tunnel surrounded by a dielectric medium, and the reflecting structure is schematically represented by a "reflecting wall." Two examples of reflecting structures are illustrated at the bottom. The first is a *nonsymmetric* structure (bottom left frame) consisting of an array of vacuum cylinders surrounding the central one; this structure is better known as a photonic band gap (PBG) structure (see Ref. [4]). Another example is an azimuthally symmetric Bragg structure (bottom right frame) consisting of a series of concentric dielectric layers. Both structures and other variants have been investigated in the context of optics applications (e.g., [5,6]); therefore, we shall skip here the analysis of propagation of homogeneous waves and limit the discussion to the effect of *nonhomogeneous* waves linked to the motion of a point charge in the central bore.

For this purpose we introduce a cylindrical coordinate system whose z axis coincides with the axis of the central vacuum tunnel. With this coordinate system it is possible to attribute to a charge q moving at a constant velocity v parallel to the z axis and located in the transverse plane at $r = r_0$ and $\phi = \phi_0$ a current density $J_z(r, z, \phi, t) = -qv(1/r)\delta(r-r_0)\delta(\phi-\phi_0)\delta(z-vt)$. In the *absence* of the dielectric structure this current density generates a (primary) field which satisfies the nonhomogeneous wave equation

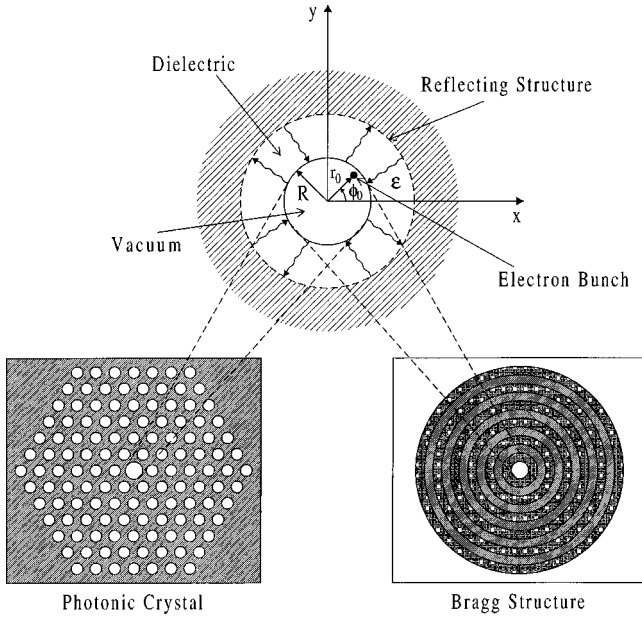


FIG. 1. Top: Schematic of the system under investigation. A point charge (q) located at $r=r_0$ and $\phi=\phi_0$ moves parallel to the z axis at a velocity v in a vacuum tunnel of radius R . The latter is surrounded by a dielectric structure that confines the electromagnetic mode. The confinement may be provided by a photonic band gap structure (bottom left), a Bragg structure (bottom right), or some other similar structure.

$$\left[\nabla^2 - \frac{1}{c^2} \frac{\partial^2}{\partial t^2} \right] A_z^{(p)}(r, z, \phi, t) = -\mu_0 J_z(r, z, \phi, t). \quad (1)$$

Its solution can be expressed as

$$A_z^{(p)}(r, z, \phi, t) = \int_{-\infty}^{\infty} d\omega e^{j\omega(t-z/v)} \sum_{n=-\infty}^{\infty} e^{jn(\phi-\phi_0)} \alpha_n(r, \omega) \quad (2)$$

with the amplitude $\alpha_n(r, \omega)$ being a solution of the following differential equation:

$$\left[\frac{1}{r} \frac{d}{dr} r \frac{d}{dr} - \frac{n^2}{r^2} - \frac{\omega^2}{c^2} \frac{1}{\gamma^2 \beta^2} \right] \alpha_n(r, \omega) = \frac{q\mu_0}{(2\pi)^2} \frac{\delta(r-r_0)}{r}. \quad (3)$$

The solution is

$$\alpha_n(r, \omega) = -\frac{q\mu_0}{(2\pi)^2} \begin{cases} K_n(\Gamma r) I_n(\Gamma r_0), & r > r_0, \\ I_n(\Gamma r) K_n(\Gamma r_0), & r < r_0, \end{cases} \quad (4)$$

with $\Gamma \equiv (|\omega|/c)(1/\gamma\beta)$.

Subsequently, the solution of the electromagnetic problem requires imposition of continuity of the tangential field components at $r=R > r_0$; therefore the corresponding primary components are presented next:

$$\begin{pmatrix} E_z^{(p)} \\ E_\phi^{(p)} \\ H_z^{(p)} \\ H_\phi^{(p)} \end{pmatrix} = -\frac{q\mu_0}{(2\pi)^2} \int_{-\infty}^{\infty} d\omega e^{j\omega(t-z/v)} \sum_{n=-\infty}^{\infty} e^{jn(\phi-\phi_0)} \times I_n(\Gamma r_0) \begin{pmatrix} \frac{j\omega}{\gamma^2 \beta^2} K_n(\Gamma r) \\ \frac{j\omega}{\left(\frac{\omega}{c} r\right) \beta} K_n(\Gamma r) \\ 0 \\ -\frac{\Gamma}{\mu_0} \dot{K}_n(\Gamma r) \end{pmatrix}. \quad (5)$$

The overdot represents the derivative with respect to the argument of the function.

III. SECONDARY FIELD

This primary field is valid in the central vacuum tunnel of the structure in the absence of the surrounding structure. The latter's effect on the field in this tunnel ($r < R$) is referred to as the secondary field and it is determined by two longitudinal components of the electromagnetic (e.m.) field:

$$\begin{pmatrix} E_z^{(s)} \\ H_z^{(s)} \end{pmatrix} = -\frac{q\mu_0}{(2\pi)^2} \int_{-\infty}^{\infty} d\omega e^{j\omega(t-z/v)} \sum_{n=-\infty}^{\infty} e^{jn(\phi-\phi_0)} I_n(\Gamma r) \times \begin{pmatrix} \frac{j\omega}{\gamma^2 \beta^2} A_n \\ -\Gamma \\ \frac{-\Gamma}{\mu_0 \gamma^2 \beta^2} B_n \end{pmatrix}, \quad (6)$$

whereas in the dielectric region ($r > R$), the secondary field is given by

$$\begin{pmatrix} E_z^{(s)} \\ H_z^{(s)} \end{pmatrix} = -\frac{q\mu_0}{(2\pi)^2} \int_{-\infty}^{\infty} d\omega e^{j\omega(t-z/v)} \sum_{n=-\infty}^{\infty} e^{jn(\phi-\phi_0)} \times \begin{pmatrix} \frac{j\omega}{\gamma^2 \beta^2} [C_n H_n^{(2)}(\Lambda r) + D_n H_n^{(1)}(\Lambda r)] \\ \frac{\Lambda}{\mu_0 \gamma^2 \beta^2} [E_n H_n^{(2)}(\Lambda r) + F_n H_n^{(1)}(\Lambda r)] \end{pmatrix}. \quad (7)$$

Note that for $\omega < 0$ the Hankel functions reverse roles, $H_n^{(2)}(u) \rightarrow H_n^{(1)}(u)$ and $H_n^{(1)}(u) \rightarrow H_n^{(2)}(u)$; $\Lambda \equiv (|\omega|/c) \sqrt{\epsilon_r - \beta^{-2}}$. If this first dielectric layer were infinite, the amplitudes (D_n, F_n) of the reflected waves would vanish. The photonic band gap structure or the Bragg structure surrounding the vacuum tunnel or any other structure that is attached to this dielectric layer causes a reflection process that in principle may couple between the TM mode represented by $E_z^{(\text{sec})}$ and the TE mode represented by $H_z^{(\text{sec})}$.

By virtue of the linearity of Maxwell's equations the amplitudes of the reflected waves may be expressed in matrix form (at $r=R$ and for $\omega>0$) as

$$\begin{pmatrix} D_n H_n^{(1)}(\Lambda R) \\ F_n H_n^{(1)}(\Lambda R) \end{pmatrix} = \sum_m \begin{pmatrix} R_{nm}^{(11)} & R_{nm}^{(12)} \\ R_{nm}^{(21)} & R_{nm}^{(22)} \end{pmatrix} \begin{pmatrix} C_m H_m^{(2)}(\Lambda R) \\ E_m H_m^{(2)}(\Lambda R) \end{pmatrix}. \quad (8)$$

Explicitly, $R_{nm}^{(11)}$ couples between the amplitudes of the incoming and outgoing TM waves, and similarly $R_{nm}^{(22)}$ couples between the amplitudes of the incoming and outgoing TE wave. Since in principle azimuthal variations are possible in this structure due to either current excitation or geometric asymmetries these two modes are coupled. In the framework of the present formulation this coupling is described by the two off-diagonal matrices: $R_{nm}^{(12)}$ couples between the amplitudes of the incoming TE mode and the outgoing amplitudes of the TM wave. In a similar way, $R_{nm}^{(21)}$ couples between the amplitudes of the incoming TM mode and the outgoing ones of the TE wave. For an azimuthally symmetric structure and excitation the TE and TM modes are decoupled, or explicitly $R^{(12)}$ and $R^{(21)}$ are identically zero. All four matrices comprise all geometric and electrical properties of the structure, and their characterization is essential for exact evaluation of the wake field. In the framework of the present study, some general assumptions will be made to account for the main features of the reflection process, analyzing their effect parametrically as well as based on a specific numerical calculation.

In order to determine the amplitudes introduced in Eqs. (6) and (7) it is necessary to establish an additional set of four equations—these are the boundary conditions for the tangential components of the field. With the longitudinal components it is possible, based on Maxwell's equations, to determine the other two tangential components in each of the regions, based on

$$\bar{E}_\phi = \frac{n}{\beta \bar{\epsilon}(\omega/c)r} \bar{E}_z - \frac{1}{j\omega \epsilon_0 \bar{\epsilon}} \frac{\partial \bar{H}_z}{\partial r},$$

$$\bar{H}_\phi = \frac{n}{\beta \bar{\epsilon}(\omega/c)r} \bar{H}_z + \frac{1}{j\omega \mu_0} \frac{\epsilon_r}{\bar{\epsilon}} \frac{\partial \bar{E}_z}{\partial r};$$

tacitly assuming that the various field components have the spatial dependence $E \sim \bar{E}(r) e^{j\omega(t-z/v)} e^{jn\phi}$ and $\bar{\epsilon} \equiv \epsilon_r - \beta^{-2}$. The explicit expressions for the azimuthal components of the electromagnetic field are presented in Appendix A.

IV. BOUNDARY CONDITIONS

By imposing the boundary conditions for the *total* tangential field components, it is possible to determine the as yet unknown amplitudes A_n , B_n , C_n , and E_n . Starting with the continuity of E_z , which entails

$$K_n(\Gamma R) I_n(\Gamma r_0) + A_n I_n(\Gamma R) = C_n H_n^{(2)}(\Lambda R) + D_n H_n^{(1)}(\Lambda R), \quad (9)$$

we proceed with the continuity of H_z leading to

$$\begin{aligned} 0 + \frac{-\Gamma}{\mu_0(\gamma\beta)^2} B_n I_n(\Gamma R) \\ = \frac{\Lambda}{\mu_0(\gamma\beta)^2} [E_n H_n^{(2)}(\Lambda R) + F_n H_n^{(1)}(\Lambda R)]. \end{aligned} \quad (10)$$

Further, continuity of E_ϕ at $r=R$ provides us with a third equation,

$$\begin{aligned} \frac{jn}{\beta(R/c)} K_n(\Gamma R) I_n(\Gamma r_0) + j\omega \left[\frac{-n}{\beta[(\omega/c)R]} A_n I_n(\Gamma R) \right. \\ \left. + \frac{1}{(\gamma\beta)^2} B_n \dot{I}_n(\Gamma R) \right] \\ = \frac{j\omega}{(\gamma\beta)^2} \left\{ \frac{n}{\beta[(\omega/c)R] \bar{\epsilon}} [C_n H_n^{(2)}(\Lambda R) + D_n H_n^{(1)}(\Lambda R)] \right. \\ \left. + E_n \dot{H}_n^{(2)}(\Lambda R) + F_n \dot{H}_n^{(1)}(\Lambda R) \right\}, \end{aligned} \quad (11)$$

and finally continuity of H_ϕ entails

$$\begin{aligned} \frac{-\Gamma}{\mu_0} \dot{K}_n(\Gamma R) I_n(\Gamma r_0) \\ + \frac{\Gamma}{\mu_0} \left[\frac{n}{\beta[(\omega/c)R]} B_n I_n(\Gamma R) - A_n \dot{I}_n(\Gamma R) \right] \\ = \frac{\Lambda \epsilon_r}{\mu_0(\gamma\beta)^2 \bar{\epsilon}} \left\{ \frac{n}{[(\omega/c)R] \beta \epsilon_r} \right. \\ \left. \times [E_n H_n^{(2)}(\Lambda R) + F_n H_n^{(1)}(\Lambda R)] \right. \\ \left. + C_n \dot{H}_n^{(2)}(\Lambda R) + D_n \dot{H}_n^{(1)}(\Lambda R) \right\}. \end{aligned} \quad (12)$$

At this stage it is convenient to adopt a matrix and vector notation for the description of the solution prescribed by Eqs. (9)–(12). Defining $\Omega \equiv \omega R/c$, $\psi \equiv \Lambda R$, $\chi = \Gamma R$, $\chi_0 = \Gamma r_0$, $\bar{A}_n \equiv A_n I_n(\chi)$, $\bar{B}_n = B_n I_n(\chi)$, $\bar{C}_n \equiv C_n H_n^{(2)}(\psi)$, $\bar{D}_n \equiv D_n H_n^{(1)}(\psi)$, $\bar{E}_n \equiv E_n H_n^{(2)}(\psi)$, and $\bar{F}_n \equiv F_n H_n^{(1)}(\psi)$, we may write based on Eq. (9)

$$\bar{A}_n = \bar{C}_n + \bar{D}_n - K_n(\chi) I_n(\chi_0). \quad (13)$$

In a similar way, Eq. (10) may be rewritten as

$$\bar{B}_n = -\gamma\beta \sqrt{\bar{\epsilon}} [\bar{E}_n + \bar{F}_n] \quad (14)$$

and based on Eq. (11), after substituting Eqs. (13) and (14),

$$M_n^{(11)} \bar{C}_n + M_n^{(12)} \bar{D}_n + M_n^{(13)} \bar{E}_n + M_n^{(14)} \bar{F}_n = S_n^{(1)}, \quad (15)$$

wherein

$$M_n^{(11)} = M_n^{(12)} \equiv \frac{n}{\beta\Omega} \left(1 + \frac{1}{\bar{\varepsilon}\gamma^2\beta^2} \right),$$

$$M_n^{(13)} \equiv \frac{1}{\gamma\beta} \sqrt{\bar{\varepsilon}} \frac{\dot{I}_n(\chi)}{I_n(\chi)} + \frac{1}{(\gamma\beta)^2} \frac{\dot{H}_n^{(2)}(\psi)}{H_n^{(2)}(\psi)},$$

$$M_n^{(14)} \equiv \frac{1}{\gamma\beta} \sqrt{\bar{\varepsilon}} \frac{\dot{I}_n(\chi)}{I_n(\chi)} + \frac{1}{(\gamma\beta)^2} \frac{\dot{H}_n^{(1)}(\psi)}{H_n^{(1)}(\psi)},$$

$$S_n^{(1)} \equiv \frac{2n}{\Omega\beta} K_n(\chi) I_n(\chi_0).$$

Following a similar approach, Eq. (12) entails

$$M_n^{(21)} \bar{C}_n + M_n^{(22)} \bar{D}_n + M_n^{(23)} \bar{E}_n + M_n^{(24)} \bar{F}_n = S_n^{(2)} \quad (16)$$

after use of the following definitions:

$$S_n^{(2)} \equiv \frac{I_n(\chi_0)}{I_n(\chi)} \frac{1}{\chi}, \quad M_n^{(21)} \equiv \frac{\varepsilon_r}{(\gamma\beta)\sqrt{\bar{\varepsilon}}} \frac{\dot{H}_n^{(2)}(\psi)}{H_n^{(2)}(\psi)} + \frac{\dot{I}_n(\chi)}{I_n(\chi)},$$

$$M_n^{(22)} \equiv \frac{\varepsilon_r}{(\gamma\beta)\sqrt{\bar{\varepsilon}}} \frac{\dot{H}_n^{(1)}(\psi)}{H_n^{(1)}(\psi)} + \frac{\dot{I}_n(\chi)}{I_n(\chi)},$$

$$M_n^{(23)} = M_n^{(24)} \equiv \frac{n}{\Omega\beta} \left(\gamma\beta\sqrt{\bar{\varepsilon}} + \frac{1}{\gamma\beta\sqrt{\bar{\varepsilon}}} \right).$$

Combining Eqs. (8), (15), and (16), it is possible to formulate the solution of the electromagnetic problem in matrix form as

$$\sum_m \begin{pmatrix} N_{nm}^{(11)} & N_{nm}^{(12)} \\ N_{nm}^{(21)} & N_{nm}^{(22)} \end{pmatrix} \begin{pmatrix} \bar{C}_m \\ \bar{E}_m \end{pmatrix} = \begin{pmatrix} S_n^{(1)} \\ S_n^{(2)} \end{pmatrix}, \quad (17)$$

which in turn relies on the next set of definitions:

$$N_{nm}^{(11)} \equiv \delta_{nm} M_m^{(11)} + M_m^{(12)} R_{nm}^{(11)} + M_m^{(14)} R_{nm}^{(21)},$$

$$N_{nm}^{(12)} \equiv \delta_{nm} M_m^{(13)} + M_m^{(12)} R_{nm}^{(12)} + M_m^{(14)} R_{nm}^{(22)},$$

$$N_{nm}^{(21)} \equiv \delta_{nm} M_m^{(21)} + M_m^{(22)} R_{nm}^{(11)} + M_m^{(24)} R_{nm}^{(21)},$$

$$N_{nm}^{(22)} \equiv \delta_{nm} M_m^{(23)} + M_m^{(22)} R_{nm}^{(12)} + M_m^{(24)} R_{nm}^{(22)}.$$

Thus formally Eq. (17) may be conceived as the solution of the electromagnetic problem since, provided the reflection matrices \mathbb{R} introduced in Eq. (8) are known, the unknown amplitudes are determined by inverting the matrix N .

V. EFFECT ON THE MOVING CHARGE

With the electromagnetic problem solved, it is possible to proceed toward determining the decelerating field on the point charge [$E_z^{(\text{sec})}$]. For this purpose, it is sufficient to calculate \bar{A}_n , which according to Eqs. (13) and (17) reads

$$A_n I_n(\chi) = -K_n(\chi) I_n(\chi_0) + \{ [I + \mathbb{R}^{(11)}] [N^{(11)} - N^{(12)} (N^{(22)})^{-1} N^{(21)}]^{-1} \times [\bar{S}^{(1)} - N^{(12)} (N^{(22)})^{-1} \bar{S}^{(2)}] + \mathbb{R}^{(12)} [N^{(22)} - N^{(21)} (N^{(11)})^{-1} N^{(12)}]^{-1} \times [\bar{S}^{(2)} - N^{(21)} (N^{(11)})^{-1} \bar{S}^{(1)}] \}_n. \quad (18)$$

Explicitly, the decelerating power is given by

$$P = \int_{-\pi}^{\pi} d\phi \int_0^R dr r \int_{-\infty}^{\infty} dz J_z(r, \phi, z, t) E_z^{(s)}(r < R, \phi, z, t) = -qv \int_{-\infty}^{\infty} d\omega \frac{j\omega}{(\gamma\beta)^2} \sum_{n=-\infty}^{\infty} A_n I_n(\chi_0) \equiv -qv \mathcal{E}_{\parallel}; \quad (19)$$

\mathcal{E}_{\parallel} denotes the decelerating field on the point charge. This expression represents a *general formulation* of the decelerating field acting on a point charge as it moves along a cylindrical vacuum tunnel bored in a dielectric medium of radius R . The reflecting structure outside the vacuum tunnel is represented by four reflection matrices \mathbb{R} introduced in Eq. (8). It is worth mentioning that the term $-K_n(\chi) I_n(\chi_0)$ in Eq. (18) represents the self-field, since it is independent of the characteristics of the confining structure or the dielectric layer; therefore it has no contribution to the decelerating power and only the term in the curly brackets may have a nonzero contribution.

VI. DECELERATING FIELD

Although the formulation so far is general and accounts for any nonsymmetric structures, such as a photonic band gap structure, for most practical purposes it may be assumed that the point charge is located on the z axis ($r_0=0$). This assumption implies that only the zero harmonic has a nonzero contribution to the longitudinal field since $I_{n \neq 0}(\Gamma r_0=0)=0$. Furthermore, subject to this assumption and for the sake of simplicity, we shall limit the formulation developed so far to an *azimuthally symmetric* case such as a Bragg structure or the contribution of the zero harmonic in a photonic band gap structure; subsequently we shall briefly discuss the contribution of nonsymmetric structures.

First, the expressions will be simplified to fit the $n=0$ case and the ultrarelativistic regime ($\gamma \rightarrow \infty$), i.e., $\chi \ll 1$. Second, since $\gamma \gg 1$, it is assumed that the main contribution to the field is from high frequencies; thus $\psi \gg 1$. Third, the matrices that couple the TM and TE modes vanish for the symmetric case, i.e., $\mathbb{R}^{(12)}=0$ and $\mathbb{R}^{(21)}=0$. Consequently, the first set of matrices introduced [Eq. (15)] are given by

$$M_0^{(11)} = M_0^{(12)} = 0, \quad M_0^{(13)} \simeq \frac{1}{\gamma} \sqrt{\bar{\varepsilon}} \frac{\chi}{2} - \frac{j}{\gamma^2},$$

$$M_0^{(14)} \simeq \frac{1}{\gamma} \sqrt{\bar{\varepsilon}} \frac{\chi}{2} + \frac{j}{\gamma^2},$$

whereas the second set reads

$$M_0^{(21)} \simeq \frac{-j\epsilon_r}{\gamma\sqrt{\epsilon}} + \frac{\chi}{2}, \quad M_0^{(22)} \simeq \frac{j\epsilon_r}{\gamma\sqrt{\epsilon}} + \frac{\chi}{2},$$

$$M_0^{(23)} = M_0^{(24)} = 0.$$

For the zero harmonic, the source term of the TE mode is zero, $S_0^{(1)} = 0$. Correspondingly, the source of the TM mode is $S_0^{(2)} = (1/\chi)[I_0(\chi_0)/I_0(\chi)] \simeq 1/\chi$. These results imply that two of the N matrices are zero, $N^{(11)} = 0$ and $N^{(22)} = 0$, whereas the other two read

$$N^{(12)} = \frac{1}{\gamma} \sqrt{\epsilon} \frac{\chi}{2} - \frac{j}{\gamma^2} + \left(\frac{1}{\gamma} \sqrt{\epsilon} \frac{\chi}{2} + \frac{j}{\gamma^2} \right) R^{(22)},$$

$$N^{(21)} = -\frac{j\epsilon_r}{\gamma\sqrt{\epsilon}} + \frac{1}{2}\chi + \left(\frac{j\epsilon_r}{\gamma\sqrt{\epsilon}} + \frac{1}{2}\chi \right) R^{(11)}.$$

Since the source term of the TE mode is zero, $S_0^{(1)} = 0$, and there is no coupling between TE and TM modes in the symmetric case, the former vanishes ($\bar{E}_n = 0$)—as one may expect. As a result, the amplitude of the TM mode is determined by

$$\begin{aligned} \bar{C}_0 &= [N_0^{(21)}]^{-1} S_0^{(2)} \\ &= \left[-\frac{j\epsilon_r}{\gamma\sqrt{\epsilon}} + \frac{1}{2}\chi + \left(\frac{j\epsilon_r}{\gamma\sqrt{\epsilon}} + \frac{1}{2}\chi \right) R^{(11)} \right]^{-1} \frac{1}{\chi}; \end{aligned}$$

thus, after defining $\bar{\omega} \equiv \frac{1}{2}\chi\gamma\sqrt{\epsilon}/\epsilon_r = \Omega\sqrt{\epsilon}/2\epsilon_r$, the effect of the reflection process is revealed in the explicit expression for the decelerating field,

$$\mathcal{E}_{\parallel} = \frac{q}{4\pi\epsilon_0 R^2} \frac{2}{\pi} \int_{-\infty}^{\infty} d\bar{\omega} \frac{1 + R^{(11)}(\bar{\omega})}{1 + j\bar{\omega} - (1 - j\bar{\omega})R^{(11)}(\bar{\omega})}. \quad (20)$$

It warrants mention that if $\psi \gg 1$ is not satisfied then

$$\mathcal{E}_{\parallel} = \frac{q}{4\pi\epsilon_0 R^2} \frac{2}{\pi} \int_{-\infty}^{\infty} d\bar{\omega} \frac{1 + R^{(11)}(\bar{\omega})}{\kappa + j\bar{\omega} - (\kappa^* - j\bar{\omega})R^{(11)}(\bar{\omega})}, \quad (21)$$

wherein $\kappa(\bar{\omega}) \equiv -jH_1^{(2)}(2\epsilon\bar{\omega})/H_0^{(2)}(2\epsilon\bar{\omega})$. After the general formulation for the decelerating field as presented in Eqs. (18) and (19), the expression in Eqs. (20) or (21) is the next most important result of this study. Its importance is a direct consequence of the possibility of establishing the wake in a structure based on a prior calculation of the reflection coefficient [$R^{(11)}$]. This calculation can be either numerical, e.g., based on HFSS or MAFIA, or analytic, on which we shall focus in what follows.

Case 1

In the absence of reflections, i.e., $R^{(11)} = 0$,

$$\mathcal{E}_{\parallel} = \frac{q}{4\pi\epsilon_0 R^2} \times \frac{4}{\pi} \int_0^{\infty} d\bar{\omega} \frac{1}{1 + \bar{\omega}^2} = \frac{q}{4\pi\epsilon_0 R^2} \times 2, \quad (22)$$

which is identical to the result reported in Ref. [7].

Case 2

Another insight is disclosed by defining the normalized impedance as $\bar{Z}_{\text{in}} \equiv (1 + R^{(11)})/(1 - R^{(11)})$. It allows formulation of the decelerating field in terms of the impedance experienced by the wave propagating outward, namely,

$$\mathcal{E}_{\parallel} = \frac{q}{4\pi\epsilon_0 R^2} \times \frac{2}{\pi} \int_{-\infty}^{\infty} d\bar{\omega} \frac{\bar{Z}_{\text{in}}}{1 + j\bar{\omega}\bar{Z}_{\text{in}}} = \frac{q}{4\pi\epsilon_0 R^2} \times 2. \quad (23)$$

If this impedance happens to be frequency independent and has zero imaginary component, the deceleration field is independent of its exact value. However, the situation is different when the impedance has resonances.

Case 3

In order to account for the effect of reflections, consider a perfect reflector that imposes $E_z(r = R_{\text{ext}} > R) = 0$, for which the reflection coefficient is

$$R^{(11)} = -\frac{H_0^{(2)}(\Lambda R_{\text{ext}}) H_0^{(1)}(\Lambda R)}{H_0^{(1)}(\Lambda R_{\text{ext}}) H_0^{(2)}(\Lambda R)} \simeq -e^{-2j\bar{\omega}\delta r}, \quad (24)$$

wherein for the expression in the right-hand side it is tacitly assumed that $\Lambda R \gg 1$ and $\delta r \equiv 2\epsilon_r(R_{\text{ext}} - R)/R$; this last parameter represents the normalized distance where reflections occur. In Appendix B it is demonstrated that, regardless of the value of δR , the decelerating field on the point charge is identical to the case when no reflection occurs—i.e., Eq. (22). In other words, a (Čerenkov) wave emitted by the charge and being reflected by the discontinuity reaches the axis after the point charge has passed there and, as a result, the *bunch is not affected by the discontinuity* at $r = R_{\text{ext}}$.

Case 4

It is a well known fact that perfect reflection from this “ideal wall” leads to an infinite number of modes [8]. Accordingly, it is possible to account for the effects of a structure that supports a *single mode*, as in the case of a highly symmetric photonic band gap structure, by “filtering” out all the modes except one. Based on this metallic wall model, this filtering process may be understood in terms of having a wall made of a frequency-dependent metal. The reflection coefficient in this case may be assumed to be given by $R^{(11)} \simeq -\rho(\bar{\omega})e^{-2j\bar{\omega}\delta r}$ wherein

$$\rho(\bar{\omega}) \simeq \rho_0 \frac{e^{-[(\bar{\omega} - \bar{\omega}_0)/\delta\omega]^2} + e^{-[(\bar{\omega} + \bar{\omega}_0)/\delta\omega]^2}}{1 + e^{-(2\bar{\omega}_0/\delta\omega)^2}}, \quad (25)$$

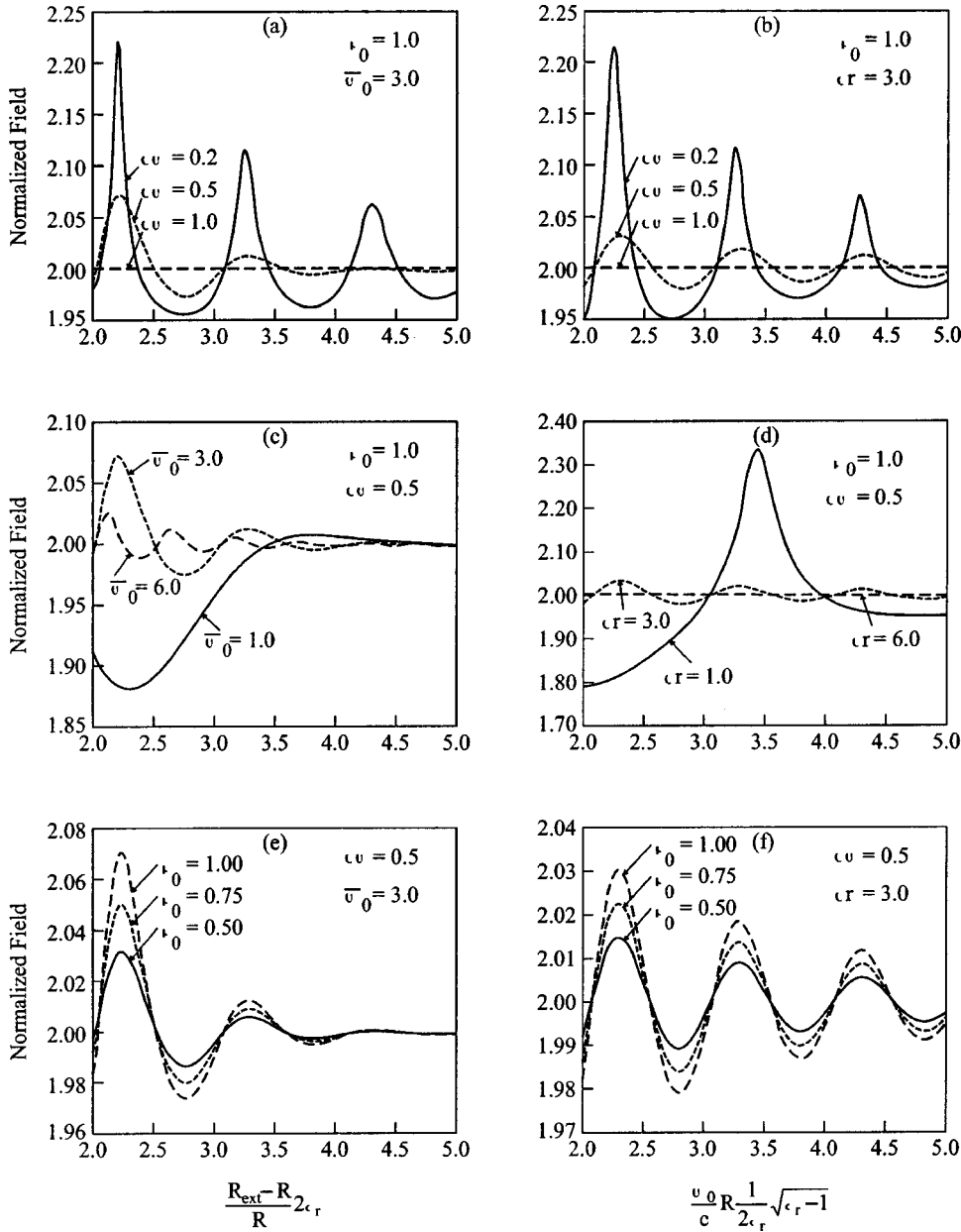


FIG. 2. The normalized decelerating field $\mathcal{E}_{\parallel}(q/4\pi\epsilon_0 R^2)^{-1}$, as a function of the normalized distance where reflections occur, $\delta r = 2\epsilon_r(R_{\text{ext}} - R)/R$ (left column). In the right column, the same quantity is plotted as a function of normalized frequency $\bar{\omega} = (\omega_0/c)R(1/2\epsilon_r)\sqrt{\epsilon_r - 1}$; $\delta\omega = (\Delta\omega/c)R(1/2\epsilon_r)\sqrt{\epsilon_r - 1}$ is the bandwidth of the reflection.

$\rho(\bar{\omega})$ being a real defined function whose maximum value is ρ_0 , which occurs at $|\bar{\omega}| = \bar{\omega}_0$, and the width of the peak being $\delta\omega$. Further assuming that $\rho(\bar{\omega})$ is relatively narrow, i.e., $\bar{\omega}_0 \gg \delta\omega$, we get

$$\mathcal{E}_{\parallel} \approx \frac{q}{4\pi\epsilon_0 R^2} \times \left\{ 2 + \frac{4}{\pi} \int_{\bar{\omega}_0 - 3\delta\omega}^{\bar{\omega}_0 + 3\delta\omega} d\bar{\omega} \operatorname{Re} \left[\frac{1 + R^{(11)}}{1 + j\bar{\omega} - (1 - j\bar{\omega})R^{(11)}} - \frac{1}{1 + j\bar{\omega}} \right] \right\}; \quad (26)$$

note that the integration is limited to six times the bandwidth of the reflection coefficient because of the exponential decay associated with it. This integral can be evaluated numerically (Fig. 2), illustrating the dependence of the normalized decelerating field [$\bar{\mathcal{E}}_{\parallel} \equiv \mathcal{E}_{\parallel}/(q/4\pi\epsilon_0 R^2)$] on the four main parameters of the model: (i) the maximum reflection coefficient

(ρ_0), (ii) the normalized resonance frequency of the reflecting wall [$\bar{\omega}_0 \equiv (\omega_0/c)R\sqrt{\epsilon_r - 1}/(1/2\epsilon_r)$], (iii) the reflection bandwidth of the structure [$\delta\omega \equiv (\Delta\omega_0/c)R\sqrt{\epsilon_r - 1}/(1/2\epsilon_r)$], and (iv) the normalized distance where the reflection occurs [$\delta r = [(R_{\text{ext}} - R)/R]2\epsilon_r$]. All three frames in the left column show that the effect of reflections (from $r = R_{\text{ext}}$) on the point charge diminishes as the separation parameter δr increases. In fact, all three frames demonstrate that the normalized field *decays exponentially* to its asymptotic value [see Eq. (21)] as a function of this parameter. This may be understood in terms of the time it takes the photon emitted by the point charge to reach the reflecting surface. The further away this surface is, the lower the probability becomes that the reflected photon acts back on the particle. A similar, but not as pronounced, behavior is revealed by the frames in the right column which illustrate the normalized field as a function of normalized

resonant frequency ($\bar{\omega}_0$) of the reflecting structure. In other words, for most practical cases if $(R_{\text{ext}} - R)/R \geq 2/\epsilon_r$ the decelerating field (and thus the wake) is *independent* of the geometric or electric properties of the reflecting structure and is given by $\mathcal{E}_{\parallel} = (q/4\pi\epsilon_0 R^2) \times 2$ —as already indicated in case 3.

Focusing next on frames (a) and (b), we observe that the bandwidth of the reflecting structure has a very strong impact if δr is relatively small. When the bandwidth is much smaller than the resonant frequency (or in normalized units $\delta\omega \ll \bar{\omega}_0$), then the point charge may experience a decelerating field that is 10% larger than in the absence of reflections. Regardless of the value of the bandwidth, for sufficiently large δr and $\bar{\omega}_0$ the decelerating field decays to its asymptotic value; in all these cases $\rho_0 = 1$. Frames (c) and (d) reveal the oscillatory as well as the decaying character of the decelerating field; for most practical purposes, the contribution seems to be limited to less than 10%. This conclusion is valid also when δr is a parameter, except if the latter is relatively small [$(R_{\text{ext}} - R)/R \leq 1/2\epsilon_r$], in which case the decelerating field may be larger by more than 15% compared to the asymptotic value.

Frames (e) and (f) reveal the impact of the reflection coefficient on the decelerating field. It is evident that ρ_0 has no effect on the oscillation's frequency but it affects its amplitude quite significantly. The maximum effect occurs when the reflection coefficient is unity; however, there is a significant effect even if there is only partial reflection. In other words, even if the structure does not support the propagation of a mode synchronous with a relativistic particle, there is a non-negligible effect of the reflecting structure on a moving point charge. For the parameters presented here ($\delta\omega = 0.5$ and $\bar{\omega}_0 = 3$ or $\delta r = 3$) the variation is less than 2%.

Case 5

Another topic that needs to be addressed is the impact of the wake generated by a single bunch on trailing bunches. For this purpose one needs to go back to Eq. (20) and rewrite it including the corresponding delay term, namely,

$$\begin{aligned} \mathcal{E}_{\parallel}(\tau = t - z/v) &= \frac{q}{4\pi\epsilon_0 R^2} \frac{2}{\pi} \int_{-\infty}^{\infty} d\bar{\omega} \frac{1 + \mathbb{R}^{(11)}(\bar{\omega})}{1 + j\bar{\omega} - (1 - j\bar{\omega})\mathbb{R}^{(11)}(\bar{\omega})} e^{j\bar{\omega}\tau/\tau_0}, \\ & \quad (27) \end{aligned}$$

wherein $\tau_0 = (R/c)(1/2\epsilon_r)\sqrt{\epsilon_r - 1}$. As before, it is straightforward to evaluate the wake in the absence of reflection ($\mathbb{R}^{(11)} = 0$), and it reads [9]

$$\mathcal{E}_{\parallel}(\tau) = \frac{q}{4\pi\epsilon_0 R^2} \times f(\tau) \equiv \frac{q}{4\pi\epsilon_0 R^2} \times \begin{cases} 0, & \tau < 0, \\ 2, & \tau = 0, \\ 4e^{-\tau/\tau_0}, & \tau > 0. \end{cases} \quad (28)$$

If the structure supports an infinite number of modes, then a point charge injected in the system excites a (discrete) spectrum of angular frequencies (ω_s). The wake trailing behind the bunch *on axis* is then given by

$$\mathcal{E}_{\parallel}(\tau) = \frac{q}{4\pi\epsilon_0 R^2} \times \sum_{s=1}^{\infty} \alpha_s \cos(\omega_s \tau), \quad (29)$$

where $\alpha_s \approx (2\omega_1/2\pi) \int_0^{2\pi/\omega_1} dt f(t) \cos(\omega_s t)$ —tacitly assuming that $\omega_1 \tau_0 \ll 1$. In any event, the first eigenfrequency has to correspond to the wavelength of the driving laser field; moreover, the dielectric material making up the optical acceleration structure is frequency dependent and therefore, in practice, only a few modes are supported. Consequently, of particular interest is the case when only the *first mode* is supported, implying a field on axis of

$$\begin{aligned} \mathcal{E}_{\parallel}(\tau) &\approx \frac{q}{4\pi\epsilon_0 R^2} \times \frac{2}{\pi} \frac{2(\lambda/R)(\pi/\epsilon_r)\sqrt{\epsilon_r - 1}}{1 + [(\lambda/R)(\pi/\epsilon_r)\sqrt{\epsilon_r - 1}]^2} \\ &\quad \times \cos\left(2\pi \frac{c\tau}{\lambda}\right); \end{aligned} \quad (30)$$

it may be readily checked that the amplitude has a maximum if $(\lambda/R)(\pi/\epsilon_r)\sqrt{\epsilon_r - 1} = 1$, further implying

$$\mathcal{E}_{\parallel}^{(\text{max})}(\tau) \approx \frac{q}{4\pi\epsilon_0 R^2} \frac{2}{\pi} \cos\left(2\pi \frac{c\tau}{\lambda}\right). \quad (31)$$

Ignoring the asymmetric character of a photonic band gap structure, this last analytic result gives a reasonable estimate of the wake trailing behind the point charge in any photonic band gap structure that is uniform in the z direction.

Case 6

As already indicated, the importance of Eq. (20) stems from its ability to harness numerical calculations using e.m. software packages such as HFSS or MAFIA to determine $\mathbb{R}^{(11)}$ and evaluate the wake of complex structures. In order to demonstrate this feature, we shall consider the reflection coefficient [$\mathbb{R}^{(11)}$] of a hollow fiber based on a Bragg structure analyzed in detail elsewhere. Its absolute value is presented in Fig. 3 as a function of the (normalized) frequency for 50 interchanging dielectric layers ($\epsilon_1 = 2.1$, $\epsilon_2 = 4$) and an internal radius that is half the wavelength of the accelerating mode ($R = 0.5\lambda_0$). Although for a large fraction of the spectrum waves are transmitted through the Bragg structure, there are narrow sections where almost complete reflection occurs, the width of these regions being inversely proportional to the number of layers of the Bragg structure.

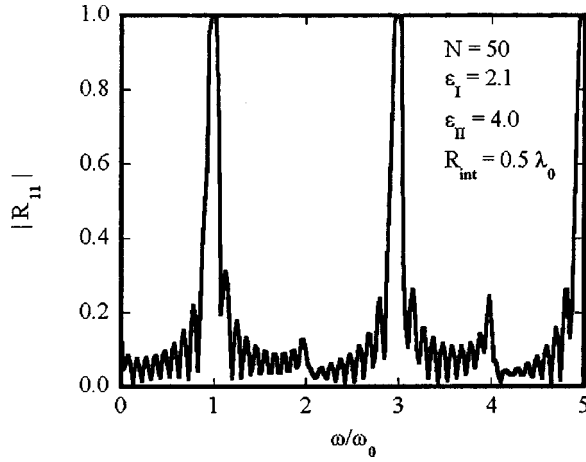


FIG. 3. Absolute value of reflection coefficient as a function of the normalized frequency ω/ω_0 .

Consider now a macrobunch consisting of M uniform microbunches of width α ($< 2\pi$) and separated by one wavelength (λ_0). Based on Eq. (27), it may be readily shown that the electromagnetic power generated by such a macrobunch is given by

$$P = \frac{-vQ^2}{4\pi\epsilon_0 R^2} \frac{2}{\pi} \int_{-\infty}^{\infty} d\bar{\omega} \frac{1 + R_{11}(\bar{\omega})}{\kappa + j\bar{\omega} - (\kappa^* - j\bar{\omega})R_{11}(\bar{\omega})} \times \text{sinc}^2\left(\frac{\alpha}{2} \frac{\bar{\omega}}{\bar{\omega}_0}\right) \frac{\text{sinc}^2[\pi M(\bar{\omega}/\bar{\omega}_0)]}{\text{sinc}^2[\pi(\bar{\omega}/\bar{\omega}_0)]}, \quad (32)$$

where $\text{sinc}(x) \equiv \sin(x)/x$, and $\bar{\omega}_0 \equiv 2\pi(R/\lambda_0)\sqrt{\epsilon - 1}/(2\epsilon)$.

A numerical evaluation of Eq. (32) is presented in Fig. 4 for Bragg structures of several numbers of layers: $N_0 = 10, 20, 30$, and 40 . It shows that in case of better confinement (larger N_0) the normalized emitted power is more moderately dependent on the number of bunches. Here is the place to mention that the frequency integral was performed up to $\bar{\omega} = 50\bar{\omega}_0$, since if $\lambda_0 \approx 1 \mu\text{m}$ then at wavelengths shorter than 30 nm the dielectric properties of the material are strongly dependent on the frequency, and for all practical purposes it becomes transparent—in other words, the contribution to the decelerating field virtually vanishes.

Case 7

Before we conclude, a comment on nonsymmetric structures is appropriate. If the point charge is on axis and the structure is *nonsymmetric*, the decelerating force is expected to have a form similar to Eq. (20) or Eq. (21). The reflection coefficient includes not only the reflection coefficient $R^{(11)}$ that couples between outgoing and incoming zero harmonics of the TM mode, but also coupling from the zero harmonic to nonzero harmonics and back to the zero harmonic, i.e.,

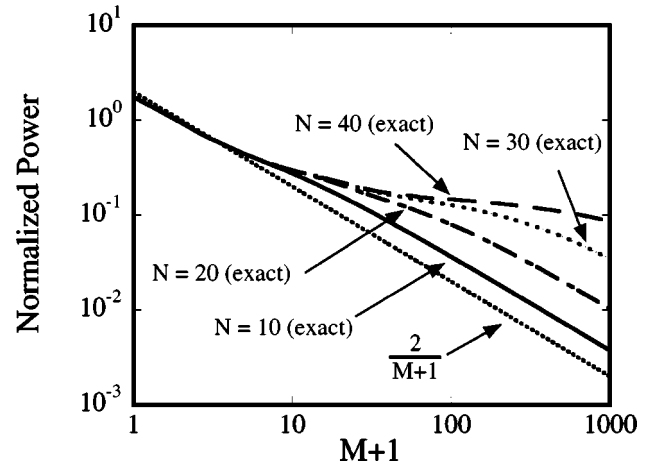


FIG. 4. Normalized power generated by a train of $M+1$ microbunches: exact calculation for $N=10, 20, 30, 40$; here $R_{\text{int}} = 0.3\lambda_0$, $\epsilon_I = 2.1$, $\epsilon_{II} = 4.0$.

$$R_{0,0}^{(11)} \rightarrow R^{(11)} = R_{0,0}^{(11)} + \sum_{n,m=-\infty}^{\infty} \mathcal{O}_{0,n}^{(1)} \mathcal{O}_{n,m}^{(2)} \mathcal{O}_{m,0}^{(3)}, \quad (33)$$

where $\mathcal{O}^{(1)}$, $\mathcal{O}^{(2)}$, and $\mathcal{O}^{(3)}$ are three operators that depend on the matrices N . The effect of reflections due to nonsymmetric modes that couple through the structure is not expected to be significantly different from the one discussed above for the zero harmonic. Obviously, the effective location of the reflection (δr) may be different, and so is the resonant frequency ($\bar{\omega}_0$) of the maximum reflection structure (ρ_0) as well as its bandwidth ($\delta\omega$). Clearly, the reflection coefficient $R^{(11)}$ for complex structures can be calculated based only on numerical methods and/or commercially available software packages. With it, the decelerating field, or the power, can be readily evaluated using Eq. (20) or Eq. (32), respectively.

VII. SUMMARY

In conclusion, a general approach was developed enabling us to estimate the impact of a dielectric structure that is uniform in the direction parallel to the moving charge and has virtually arbitrary characteristics in the transverse directions. A quasianalytic expression that relates the decelerating force to the first dielectric layer, the radius of the vacuum tunnel where the charge moves, and the reflection characteristics of the structure has been developed. The simulation results indicate that, if the effective location where the reflection occurs in the dielectric is sufficiently apart from the edge of the vacuum tunnel, it has no effect on the point charge. In fact, the decelerating field converges exponentially to its asymptotic value set by the first layer of dielectric material. An analytic estimate [Eq. (31)] of the trailing wake has been provided for the case when the electromagnetic structure (e.g., photonic band gap) supports only one mode.

ACKNOWLEDGMENTS

This study was supported by the Israel Science Foundation, the United States Department of Energy, and the Fund for the Promotion of Research at the Technion.

APPENDIX A

The azimuthal components of the secondary field in the vacuum tunnel ($r < R$) are given by

$$\begin{pmatrix} E_\phi^{(s)} \\ H_\phi^{(s)} \end{pmatrix} = -\frac{q\mu_0}{(2\pi)^2} \int d\omega e^{j\omega(t-z/v)} \sum_n e^{jn(\phi-\phi_0)} \times \left(\begin{array}{l} \frac{j\omega}{(\gamma\beta)^2} \left\{ \frac{n}{[(\omega/c)r]\beta\bar{\epsilon}} [C_n H_n^{(2)}(\Lambda r) + D_n H_n^{(1)}(\Lambda r)] + E_n \dot{H}_n^{(2)}(\Lambda r) + F_n \dot{H}_n^{(1)}(\Lambda r) \right\} \\ \frac{\Lambda \epsilon_r}{\mu_0 (\gamma\beta)^2 \bar{\epsilon}} \left\{ \frac{n}{[(\omega/c)r]\beta\epsilon_r} [E_n H_n^{(2)}(\Lambda r) + F_n H_n^{(1)}(\Lambda r)] + C_n \dot{H}_n^{(2)}(\Lambda r) + D_n \dot{H}_n^{(1)}(\Lambda r) \right\} \end{array} \right). \quad (A2)$$

APPENDIX B

The wake generated by a point charge on the axis of the structure is given by

$$\mathcal{E}_\parallel(\bar{\tau}) = \frac{Q}{4\pi\epsilon_0 R^2} \left[\frac{2}{\pi} \int_{-\infty}^{\infty} d\bar{\omega} \times \frac{1}{[1 - R^{(11)}(\bar{\omega})]/[1 + R^{(11)}(\bar{\omega})] + j\bar{\omega}} e^{j\bar{\omega}\bar{\tau}} \right], \quad (B1)$$

where $\bar{\tau} = (t-z/c)(c/R)(2\epsilon)/\sqrt{\epsilon-1}$. In the denominator, we identify the effective (normalized) impedance of the wave $\bar{Z}_{in} = (1 + R^{(11)})/(1 - R^{(11)})$. To demonstrate our statement in the context of Eq. (20), it is convenient to assume a *single* discontinuity at a distance $\Delta = R_{ext} - R$ from the vacuum-dielectric interface, and the main contribution to the integral is from wavelengths smaller than the internal radius of the structure. Thus, for the transverse impedance we adopt a transmission line model

$$\bar{Z}_{eff} = \frac{Z_2/Z_1 + j \tan[(\omega/c)\Delta\sqrt{\epsilon_1-1}]}{1 + j(Z_2/Z_1)\tan[(\omega/c)\Delta\sqrt{\epsilon_1-1}]}, \quad (B2)$$

representing a wave that propagates at a velocity $v \approx c$ along

$$\begin{pmatrix} E_\phi^{(s)} \\ H_\phi^{(s)} \end{pmatrix} = -\frac{q\mu_0}{(2\pi)^2} \int_{-\infty}^{\infty} d\omega e^{j\omega(t-z/v)} \sum_n e^{jn(\phi-\phi_0)} \times \left(\begin{array}{l} -\frac{j\omega n}{\beta[(\omega/c)r]} A_n I_n(\Gamma r) + \frac{j\omega}{(\gamma\beta)^2} B_n \dot{I}_n(\Gamma r) \\ \frac{n}{\beta[(\omega/c)r]} \frac{\Gamma}{\mu_0} B_n I_n(\Gamma r) - \frac{\Gamma}{\mu_0} A_n \dot{I}_n(\Gamma r) \end{array} \right). \quad (A1)$$

Outside the vacuum tunnel ($r \geq R$), the azimuthal field components are

the z direction, whereas the wave impedance in the medium may be shown to be given by $Z_\nu = \eta_0 \sqrt{\epsilon_\nu - 1}/\epsilon_\nu$ with $\nu = 1, 2$. Hence

$$E(\bar{\tau}) = \frac{Q}{4\pi\epsilon_0 R^2} \left[\frac{2}{\pi} \int_{-\infty}^{\infty} d\omega \frac{e^{j\bar{\omega}\bar{\tau}}}{1 + j\bar{\omega}} \times \frac{1 + \rho e^{-2j\bar{\omega}\bar{\tau}\Delta}}{1 - \rho(1 - j\bar{\omega})/(1 + j\bar{\omega})e^{-2j\bar{\omega}\bar{\tau}\Delta}} \right], \quad (B3)$$

wherein $\bar{\tau}_\Delta \equiv (\Delta/R)2\epsilon$ and $\rho = (Z_2 - Z_1)/(Z_2 + Z_1)$, which is frequency independent. With this observation and employing the explicit expression for a geometric series, we have

$$E(\bar{\tau}) = \frac{Q}{4\pi\epsilon_0 R^2} \times \left\{ \sum_{n=0}^{\infty} \rho^n \frac{2}{\pi} \int_{-\infty}^{\infty} d\omega e^{j\bar{\omega}(\bar{\tau} - 2n\bar{\tau}_\Delta)} \frac{(1 - j\bar{\omega})^n}{(1 + j\bar{\omega})^{n+1}} + \sum_{n=0}^{\infty} \rho^{n+1} \frac{2}{\pi} \int_{-\infty}^{\infty} d\bar{\omega} e^{j\bar{\omega}[\bar{\tau} - 2(n+1)\bar{\tau}_\Delta]} \frac{(1 - j\bar{\omega})^{n+1}}{(1 + j\bar{\omega})^{n+2}} \right\}, \quad (B4)$$

enabling us to determine an analytic expression for the integrals from the above:

$$\begin{aligned}
G(\bar{\tau}) &= \frac{2}{\pi} \int_{-\infty}^{\infty} d\bar{\omega} e^{j\bar{\omega}(\bar{\tau}-2m\bar{\tau}_{\Delta})} \frac{(1-j\bar{\omega})^m}{(1+j\bar{\omega})^{m+1}} \\
&= \frac{(-1)^m}{m!} \frac{2}{\pi} \left\{ \frac{d^m}{da^m} \int_{-\infty}^{\infty} d\bar{\omega} e^{j\bar{\omega}(\bar{\tau}-2m\bar{\tau}_{\Delta})} \frac{(1-j\bar{\omega})^m}{a+j\bar{\omega}} \right\} \\
&= \frac{(-1)^m}{m!} 4 \left\{ \frac{d^m}{da^m} \frac{1}{2\pi j} \int_{-\infty}^{\infty} d\bar{\omega} e^{j\bar{\omega}(\bar{\tau}-2m\bar{\tau}_{\Delta})} \right. \\
&\quad \left. \times \frac{(1-j\bar{\omega})^m}{\bar{\omega}-ja} \right\}_{a=1}. \tag{B5}
\end{aligned}$$

The integral in the curly brackets can be evaluated using Cauchy's residue theorem, defining $\theta_m \equiv \bar{\tau} - 2m\bar{\tau}_{\Delta}$,

$$\begin{aligned}
F_m(\theta_m) &\equiv \frac{1}{2\pi j} \int_{-\infty}^{\infty} d\bar{\omega} e^{j\bar{\omega}\theta_m} \frac{(1-j\bar{\omega})^m}{\bar{\omega}-ja} \\
&= e^{-a\theta_m} (1+a)^m h(\theta_m), \tag{B6}
\end{aligned}$$

wherein $h(x)$ is the Heaviside step function. Consequently,

$$\begin{aligned}
E(\bar{\tau}) &= \frac{Q}{4\pi\epsilon_0 R^2} \times \left\{ 4 \sum_{n=0}^{\infty} \rho^n h(\bar{\tau}-2n\bar{\tau}_{\Delta}) \frac{(-1)^n}{n!} \right. \\
&\quad \times \left[\frac{d^n}{da^n} e^{-a(\bar{\tau}-2n\bar{\tau}_{\Delta})} (1+a)^n \right]_{a=1} \\
&\quad + 4 \sum_{n=0}^{\infty} \rho^{n+1} h[\bar{\tau}-2(n+1)\bar{\tau}_{\Delta}] \frac{(-1)^{n+1}}{(n+1)!} \\
&\quad \left. \times \left[\frac{d^{n+1}}{da^{n+1}} e^{-a[\bar{\tau}-2(n+1)\bar{\tau}_{\Delta}]} (1+a)^{n+1} \right]_{a=1} \right\}. \tag{B7}
\end{aligned}$$

The Heaviside step functions in this expression clearly reveal that the first contribution of the *discontinuity* on the moving point charge occurs with a delay $2(\Delta/c)\sqrt{\epsilon-1}$; therefore, at $\tau=0$, the decelerating field is determined only by the vacuum-dielectric discontinuity.

-
- [1] Y. C. Huang, D. Zheng, W. M. Tulloch, and R. L. Byer, *Appl. Phys. Lett.* **68**, 753 (1996); Y. C. Huang and R. L. Byer, *ibid.* **69**, 2175 (1996); Y. C. Huang *et al.*, *Nucl. Instrum. Methods Phys. Res. A* **407**, 316 (1998); R. L. Byer *et al.*, in *Proceedings of the Particle Accelerator Conference, Piscataway, NJ, 1999* (IEEE, New York, 1999), Vol. 5, p. 3778.
- [2] S. A. Heifets and S. A. Kheifets, *Rev. Mod. Phys.* **63**, 631 (1991).
- [3] A. W. Chao, *Physics of Collective Beam Instabilities in High Energy Accelerators* (Wiley, New York, 1993), pp. 1–126; A. W. Chao and M. Tigner, *Handbook of Accelerator Physics and Engineering* (World Scientific, Singapore, 1999), pp. 194–212.
- [4] X. E. Lin, *Phys. Rev. ST Accel. Beams* **4**, 051301 (2001).
- [5] P. Yeh, A. Yariv, and E. Marom, *J. Opt. Soc. Am.* **68**, 1196 (1978); Y. Xu, R. K. Lee, and A. Yariv, *Opt. Lett.* **25**, 1756 (2000).
- [6] Y. Fink, D. J. Ripin, S. Fan, C. Chen, J. D. Joannopoulos, and E. L. Thomas, *J. Lightwave Technol.* **17**, 2039 (1999); S. G. Johnson, M. Ibanescu, M. Skorobogatiy, O. Weisberg, T. D. Engeness, M. Soljacic, S. A. Jacobs, J. D. Joannopoulos, and Y. Fink, *Opt. Express* **9**, 748 (2001).
- [7] L. Schächter and D. Schieber, *Nucl. Instrum. Methods Phys. Res. A* **388**, 8 (1997).
- [8] George Dome, in *Proceedings of the European Particle Accelerator Conference, Nice, France 1990* (Editions Frontiers, Paris, 1990), p. 628.
- [9] L. Schächter, R. L. Byer, and R. H. Siemann, in *Advanced Accelerator Concepts*, edited by C. E. Clayton and P. Muggli, AIP Conf. Proc. No. 647 (AIP, Melville, NY, 2002), p. 310.